

# Role of Water Vapor in the Partial Oxidation of Propene

Y. A. Saleh-Alhamed,<sup>1</sup> R. R. Hudgins, and P. L. Silveston<sup>2</sup>

*Department of Chemical Engineering, University of Waterloo, Waterloo, Ontario N2L 3G1, Canada*

Received September 7, 1994; revised January 31, 1996; accepted February 5, 1996

The role of water vapor was explored for the partial oxidation of propene over antimony–tin–vanadium oxide (SB/Sn/V oxide) catalyst at 1 atm pressure and 340°C using a microcatalytic packed bed reactor. Steady-state, transient kinetics, TPD, and isotopic transient experiments were performed. Water suppresses the formation of CO<sub>2</sub> by blocking the most active sites which are responsible for CO<sub>2</sub> formation but water also enhances the rate of the catalytic oxidation by keeping the catalyst surface at a high oxidation state and preventing the formation of strongly bonded oxygenates. Isotopic transient experiments with labeled O<sub>2</sub> in the presence of water indicate a strong interaction between water and the catalyst surface. Water exchanges oxygen slowly with the surface of the catalyst.

© 1996 Academic Press, Inc.

## INTRODUCTION

The presence of water vapor in the reaction mixture during the selective oxidation of propene is known to improve the selectivity and depress the formation of carbon oxides. Thus, water vapor is added to the feed for the industrial production of acrolein and acrylic acid by the catalytic oxidation of propene (1). In some cases, the feed mixture may contain between 40 and 60 vol% water. One reason for adding water is to moderate temperature variation in the reactor by providing thermal “ballast.” Water also appears to influence the chemistry. The first studies on the effect of water appeared in 1962. Studies made since that time examined whether water takes part in the oxidation reaction. Also, the involvement of water in the formation of acrylic acid is documented in the literature (2). Even so, relatively little has been done to study the effect of water vapor on the kinetics of this reaction and on elucidating its role for different catalysts. This investigation addresses these questions.

## LITERATURE REVIEW

Much is known about the mechanism of propene partial oxidation. Using <sup>13</sup>C and deuterium-labeled propene,

<sup>1</sup> Current address: Chemical Engineering Department, King Abdulaziz University, P.O. Box 9027, Jeddah, 214413, Saudi Arabia.

<sup>2</sup> To whom correspondence should be addressed.

many investigators (3–7) have demonstrated that the selective oxidation of propene over a variety of oxides proceeds via the formation of a symmetrical allyl intermediate by abstraction of a hydrogen atom from a methyl group. A second hydrogen abstraction occurs with equal probability at either end of this intermediate. The rate-determining step appears to be the first hydrogen abstraction. On other catalysts, the  $\pi$ -allyl intermediate formed rapidly converts to two equivalent forms of a  $\sigma$ -allyl intermediate (8). These intermediates do not necessarily equilibrate with each other.

The existence of at least the molecular species O<sub>2</sub><sup>-</sup>, atomic O<sup>-</sup>, and O<sup>2-</sup> on the surface of the oxide is well established (9). The redox mechanism of Mars and van Krevelen is widely accepted. According to this mechanism, the cation of the catalyst is the oxidizing agent which inserts oxygen into the hydrocarbon molecule. The catalyst in turn is re-oxidized by oxygen from the gas phase. The participation of lattice oxygen (O<sup>2-</sup>) is implied, although other oxygen surface species (O<sup>-</sup> and O<sub>2</sub><sup>-</sup>) may also play a role in the oxidation of hydrocarbons. According to Haber and Grzybowska (10, 11), the nucleophilic addition of O<sup>2-</sup> brings about selective oxidation products. However, electrophilic attack by the oxygen species, O<sup>-</sup> and O<sub>2</sub><sup>-</sup>, results in the formation of epoxy or peroxy-complexes respectively. These are intermediates in the degradation of the carbon skeleton, eventually leading to total oxidation. Haber (11) mentions that the most selective catalysts are those exhibiting no isotopic oxygen exchange.

Studies using <sup>18</sup>O<sub>2</sub> tracer (12–14) showed that oxygen is directly supplied by the lattice. Sancier *et al.* (14) concluded that the oxidation of propene on bismuth molybdate involves both lattice and sorbed oxygen at low temperatures. At higher temperatures, lattice oxygen predominates due to its increased mobility. Ruckenstein *et al.* (15) found that the catalyst activity increases as the diffusion coefficient in the catalyst lattice increases. Monnier and Keulks (16) showed that the selective oxidation over bismuth molybdate involves numerous sublayers of the catalyst.

Regarding the effect of water on this reaction, early studies (17–19) using copper oxide catalysts reported an improvement in the selectivity in the presence of water vapor. Also, Polkovnikova *et al.* (19) reported an increase in propene conversion. More recent studies (20, 21) using

complex oxide catalysts showed that acrolein formation does not depend on water or oxygen partial pressures, whereas acrylic acid formation does depend on water vapor. For the partial oxidation of butane, water vapor has been reported to accelerate the evolution of the catalyst surface area (22).

Tracer studies using  $\text{H}_2^{18}\text{O}$  (23, 24) showed that on a Pd catalyst, oxygen from water was incorporated in acetone and acrolein. They suggested that the formation of acrolein involves interaction of an allylic intermediate with a surface hydroxyl originating from water. On the other hand, the low  $^{18}\text{O}$  content of the acrolein produced using an Sn/Mo oxide catalyst suggests that oxygen in the acrolein molecule originates from molecular oxygen. Incorporation of deuterium in the acetaldehyde and acrolein products was not observed during propene oxidation over Sb/Sn oxide catalyst in the presence of  $\text{D}_2\text{O}$  (25). Nováková *et al.* (2) studied the partial oxidation of propene on Mo/W/Sn/Te oxide catalyst in the presence of  $^{18}\text{O}$ -labeled water. They concluded that an acrolein-lattice oxygen complex forms and reacts further with oxygen from water to give acrylic acid.

It is evident from the above review that our knowledge of the role of water in the selective oxidation of hydrocarbons lags behind our understanding of the oxidation mechanism. The presence of water seems necessary for the formation of acrylic acid but is not necessary for acrolein formation.

## EXPERIMENTAL

### Equipment

A schematic diagram of the experimental setup is shown in Fig. 1. All gases were of prepurified grade except propene, which had 99% minimum purity. Nitrogen and oxygen were passed through filters containing molecular sieves and anhydrous calcium sulfate to reduce traces of impurities and moisture. Propene was used without pretreatment. Water vapor was introduced by bubbling nitrogen through a saturator. To avoid condensation of water and adsorption of acrylic acid, all tubing was kept at  $90^\circ\text{C}$ .

An AD/DA converter (Taurus One) was used for communicating between the field units (mass flow controller, solenoid valves, sampling valve actuators, and electronic integrators) and a microcomputer. The computer operated the mass flow controllers, chromatograph, and sample injection and turned on the chromatograph integrator. It also collected flow rate, pressure, and temperature data.

To minimize wall catalytic activity, titanium was chosen in place of stainless steel for the reactor, the preheater, and the outlet of the reactor (26). Blank runs in the titanium reactor and lines showed no catalytic activity. Feed was introduced from the top of the reactor to avoid fluidization of the catalyst bed. The catalyst (40/60 mesh particle size) was diluted with glass beads of a similar size at a ratio of

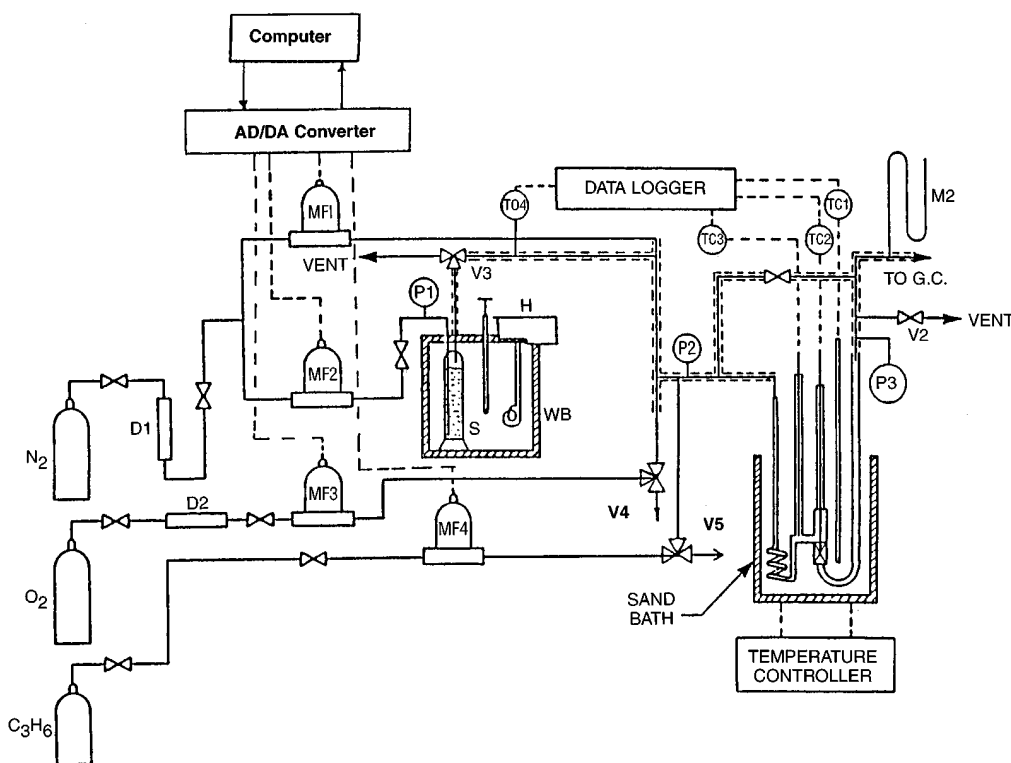


FIG. 1. Schematic of the experimental system: mass flow controllers, MF1 to MF4; water saturator, S; water bath at  $83^\circ\text{C}$ , WB; three-way solenoid valves, V3 to V5; thermocouples, TC1 to TC4; pressure gauges, P2, P3; mercury manometer, M2; drying tubes, D1, D2.

0.8 g catalyst to 1.8 g glass beads; the catalyst bed was supported between screens within the reactor. Thermocouples measured temperatures of the inlet feed, the center of the catalyst bed, and the fluidized sand bath. Titanium tubing connecting the reactor to the gas chromatograph (GC) sample valve suppressed further reactions. Design details are given by Saleh (27).

The analysis of acetaldehyde, acrolein, acetone, acetic acid, acrylic acid and propene was accomplished using a GC equipped with a flame ionization detector (FID) and a 1.3-m stainless-steel column packed with Porapak N. CO<sub>2</sub> and water were analyzed in a second GC equipped with a thermal conductivity detector (TCD) and a single column packed with Porapak Q. In this column, CO was not separable from the O<sub>2</sub>/N<sub>2</sub> peak.

### Catalyst

The Sb/Sn/V oxide catalyst used in this study was supplied by Distillers Company Limited. It had a nominal atomic composition 2/1/1, Sb/Sn/V, prepared as outlined in their 1966 British Patent 1,034,914. With this catalyst, acrolein, acetaldehyde, CO<sub>2</sub>, acetone, acrylic acid, and acetic acid are produced.

The atomic composition of the Sb/Sn/V oxide catalyst was checked by plasma emission spectrometry and agreed closely with the nominal composition given above. The BET surface area of the vanadate catalyst was measured to be 2.1 m<sup>2</sup>/g. X-ray diffraction and X-ray photoelectron spectrometric measurements were also made on both fresh catalysts. Diffraction patterns were obtained using a Siemens D500 X-ray diffraction machine with a CuK $\alpha$  (1.54060 Å) X-ray source. Using the ASTM powder diffraction files, SnO<sub>2</sub>,  $\alpha$ -Sb<sub>2</sub>O<sub>4</sub>, V<sub>2</sub>O<sub>3</sub>, and SbVO<sub>4</sub> were identified (27). The presence of V<sub>2</sub>O<sub>3</sub> is surprising but it occurs in very small amounts as indicated by weak diffraction lines in the XRD spectra. Vanadium is present mainly as antimony vanadate. Tin occurs as SnO<sub>2</sub>. Only the  $\alpha$ -modification of antimony oxide is present in the bulk of the catalyst.

X-ray photoelectron spectroscopy of used and fresh catalyst samples was carried out by the Surface Science Laboratory, University of Western Ontario, London, Ontario, on a modified Surface Science Laboratory (SSL) Model SSX-100 XPS. Spectra were collected using a 600- $\mu$ m X-ray spot size. The X-ray source was monochromatized AlK $\alpha$  X-rays (27). These measurements showed that vanadium is present as V<sup>5+</sup>, antimony as Sb<sup>5+</sup>, and tin as either Sn<sup>2+</sup> or Sn<sup>4+</sup>. Changes during catalyst use were detected and are discussed below.

## RESULTS AND DISCUSSION

Most experiments were performed at 340°C and atmospheric pressure. Propene (C<sub>3</sub><sup>-</sup>) concentrations up to 20% (by volume) at three levels of O<sub>2</sub> (5, 10, and 20%) were em-

ployed. With the O<sub>2</sub> concentration at 20%, the water dependence was also studied at two levels of C<sub>3</sub><sup>-</sup> (5 and 10%). The dependence of rate on propene and oxygen concentrations was studied at 10% H<sub>2</sub>O. Results were corrected for catalyst deactivation. Oxygen concentration was obtained from carefully calibrated gas-flow measurements. Total conversions did not exceed 10% and were usually much lower.

### Transport Interference

Criteria for the onset of transport interference (28–31) were satisfied. Indeed, numerical values were never greater than one-tenth of the published threshold values (27). Furthermore, varying the gas-flow rate established that above a total flow rate of 100 ml(STP)/min, the reaction rate was not affected by external heat or mass transfer (27). A total flow of 200 ml(STP)/min was used for all experiments.

### Catalyst Deactivation

The vanadate catalyst exhibited a slow deactivation with time-on-stream. Deactivation was monitored by running activity measurements between experimental runs using a standard mixture: 20% oxygen, 5% propene (C<sub>3</sub><sup>-</sup>), 75% N<sub>2</sub>; 20% O<sub>2</sub>, 5% C<sub>3</sub><sup>-</sup>; and 10% H<sub>2</sub>O, 65% N<sub>2</sub>. Deactivation was found to be an exponential decay function of time-on-stream with almost identical rate constants for acrolein, acetaldehyde, acetone, and CO<sub>2</sub>. The constants for acetic and acrylic acids were twice as high as those for the other products. This may be due to the formation of acrylic and acetic acids in a consecutive pathway from propene via acrolein and acetaldehyde.

The X-ray diffraction pattern was essentially the same for fresh samples and those exposed for long periods to the feed mixture. However, XPS measurements indicated that changes occurred in the catalyst with use. The first of these was the increase in carbon content. Carbon was found in the fresh catalyst, apparently arising from the use of graphite as a binder in pelletizing. Carbon content was significantly higher for the used catalyst. This suggests that fouling by carbon deposits may have been the cause of catalyst deactivation. Used catalyst samples also exhibited considerable change in surface antimony content at the expense of oxygen content. This suggests that the catalyst surface is reduced as a result of partial oxidation. The XPS measurements show the catalyst surface is enriched with antimony compared to the bulk composition. Surface enrichment with antimony upon calcination at high temperature (750°C) has been reported by Volta *et al.* (32).

### Influence of Feed Composition

Figure 2 shows the rate of formation of products vs propene concentration at 10% oxygen with and without water in the feed. Substantial differences in the kinetics are evident. Without water in the feed (Fig. 2a), reaction orders

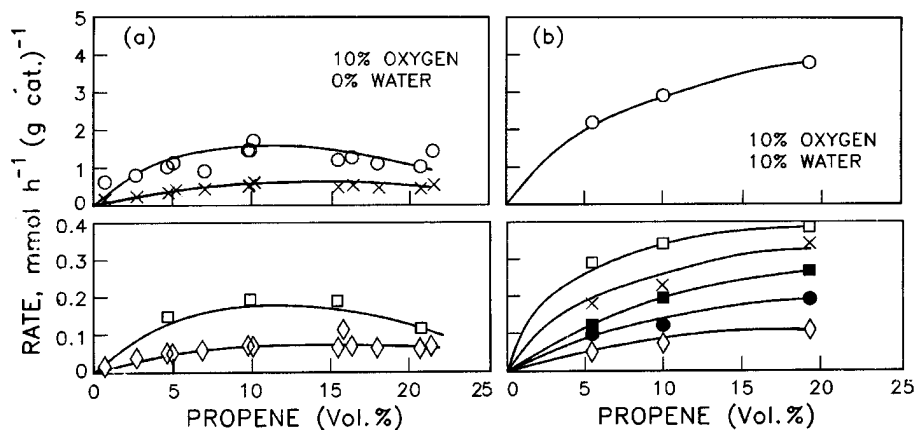


FIG. 2. Rate of formation of reaction products as a function of propene concentration with 10% oxygen at 340°C (a) without water and (b) with 10% water ◇, acetaldehyde; ●, acetic acid; ■, acetone; ○, acrolein; □, acrylic acid; ×, CO<sub>2</sub>.

for rates of formation of acrolein and acrylic acid become negative above 10% C<sub>3</sub><sup>2-</sup>. At concentrations below 10% C<sub>3</sub><sup>2-</sup>, the rate of acrolein formation is above half-order in propene. Similar behavior was also observed at 20% oxygen in the feed; however, the formation of acrolein became zero-order at propene concentrations higher than 10%. As can be seen in Fig. 2a, measurements were repeated several times with good agreement, so the conclusions about change in reaction order with propene concentration are reliable. Reproducibility was also measured in our study and found to be ±10% for acrolein and ±25% for acrylic acid.

With water present (Fig. 2b), there is no change in reaction order as the propene concentration increases. Experiments at 20 and 5% O<sub>2</sub> in the presence of 10% water vapor also indicated no change in order. The rate of formation of acrylic acid in the presence of water vapor is approximately

twice as great as in its absence and its rate of formation continues to grow with an increase in propene concentration. The formation of CO<sub>2</sub> was strongly suppressed, again by a factor of about two. Acetone is formed only in the presence of water in the feed.

Product yields vs the C<sub>3</sub><sup>2-</sup>/O<sub>2</sub> ratio with and without water are shown in Fig. 3. Yield of a particular product is defined as moles of that product per mole of propene consumed. Water has almost no effect on the acrolein and acrylic acid yields, but clearly suppresses the yields of acetaldehyde and CO<sub>2</sub>. Instead of increasing as the C<sub>3</sub><sup>2-</sup>/O<sub>2</sub> ratio increases, CO<sub>2</sub> decreases when water is present. Yields of acetaldehyde, acetic acid, and CO<sub>2</sub> in the presence of water fall at the same rate with respect to the C<sub>3</sub><sup>2-</sup>/O<sub>2</sub> ratio. This suggests that these three products are formed from a common intermediate. Furthermore, from Fig. 3b, the CO<sub>2</sub> yield is about equal to the sum of yields of acetic acid and acetaldehyde. This

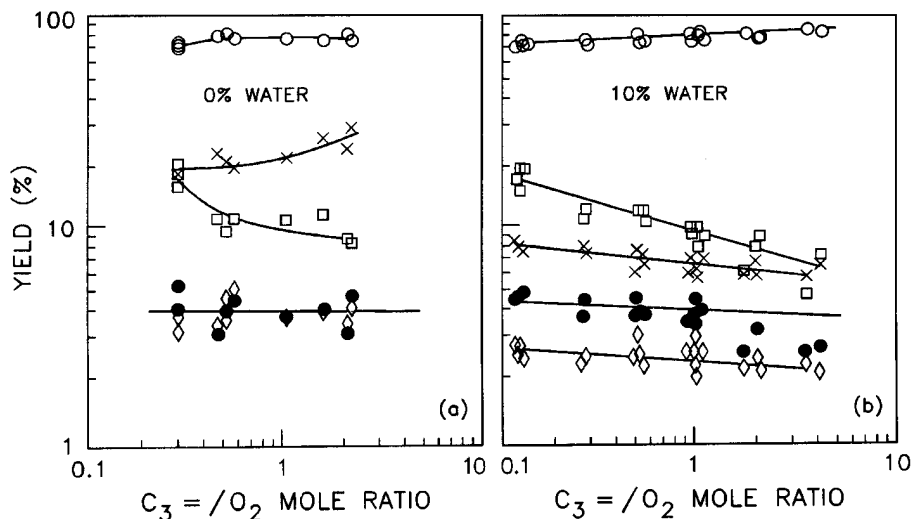


FIG. 3. Yield (%) of reaction products as a function of propene/oxygen ratio at 340°C (a) without water and (b) with 10% water in feed. Symbols as in Fig. 2.

suggests that in the presence of water, CO<sub>2</sub> together with acetaldehyde and acetic acid arises entirely from C–C bond scission. In contrast, in the absence of water, the yields of acetaldehyde and acetic acid sum to less than half of the CO<sub>2</sub> yield. The opposing trends of the CO<sub>2</sub> and acrylic acid yields with the C<sub>3</sub><sup>2-</sup>/O<sub>2</sub> ratio indicate that CO<sub>2</sub> arises from the further oxidation of acrylic acid. Thus, with water absent, more than half the CO<sub>2</sub> arises from product degradation.

With water in the feed (Fig. 3b), the yield of acrolein increases by the same percentage as the yield of acrylic acid decreases over the range of C<sub>3</sub><sup>2-</sup>/O<sub>2</sub> ratios studied. Acrylic acid must be formed from acrolein or from a common intermediate. In the presence of water vapor, the ratio of acrylic acid to acrolein is ca. 0.25 for the lowest C<sub>3</sub><sup>2-</sup>/O<sub>2</sub> ratio used (0.12). Without water, this value of the ratio was measured at C<sub>3</sub><sup>2-</sup>/O<sub>2</sub> = 0.3, again the lowest C<sub>3</sub><sup>2-</sup>/O<sub>2</sub> ratio used. Increasing the C<sub>3</sub><sup>2-</sup>/O<sub>2</sub> ratio decreases the acrylic acid/acrolein ratio. Thus, an O<sub>2</sub>-rich surface is necessary for acrylic acid formation. Unless water is present, this O<sub>2</sub>-rich surface condition results in product degradation. The different trends for acrolein, acetaldehyde, acetic acid, and CO<sub>2</sub> with the C<sub>3</sub><sup>2-</sup>/O<sub>2</sub> ratio suggest that different sites are involved for H-abstraction, O-insertion, and C–C bond scission.

The dependence of the rate of product formation on water concentration at 20% O<sub>2</sub> and 10% propene is shown in Fig. 4. A common feature for all reaction products, except for acetone, is that their rates of formation become

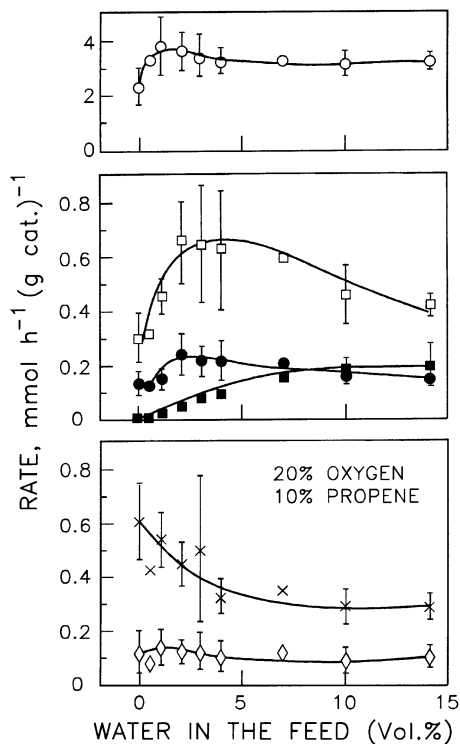


FIG. 4. Rate of formation of reaction products as a function of water concentration at 20% O<sub>2</sub> and 10% C<sub>3</sub><sup>2-</sup> at 340°C. Symbols as in Fig. 2.

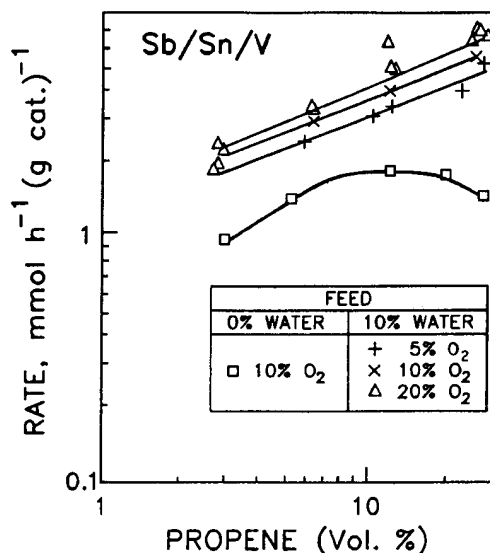


FIG. 5. Dependence of the rate of propene consumption on propene concentration with and without water at 340°C.

independent of or are slightly inhibited by water for concentrations greater than 5% water. The rate of formation of acrylic acid passes through a maximum at ca. 3 to 4% water. The existence of a maximum indicates that water must be adsorbed on sites where acrylic acid is formed or stored. The dependence of acetic acid on water concentration is similar to the dependence of acrylic acid. The rate of formation of acrolein increases sharply with the addition of small amounts of water and passes through a maximum at ca. 1% water in the feed. The acetaldehyde behavior with water content seems to be similar. The water dependence of product formation at 5% propene and 20% O<sub>2</sub> was qualitatively similar.

The strong influence of water vapor on the rates of oxygenate formation at low-water-vapor levels (1 to 20%) and the rate maxima observed as the water content of the feed increases suggests that water plays two roles on the vanadate surface. The first is to create new sites for O-insertion into the adsorbed allyl intermediate, while the second is site blockage. We speculate from the immediate reduction in the rate of CO<sub>2</sub> formation at low water levels (Fig. 4) that blockage of a site for total oxidation by one or more water molecules creates a site capable of O-insertion and thus partial oxidation.

The increasing formation of acetone with increasing water vapor indicates the existence of a parallel reaction route involving direct hydration of adsorbed propene or a surface intermediate. This route, occurring on a separate set of sites, should not affect the formation of the other oxygenates. Acetone rate dependence was less than first order in propene.

Figure 5 illustrates the rate of propene consumption vs propene concentration at different levels of oxygen with

TABLE 1  
Reaction Orders with Respect to Oxygen and Propene Concentrations with and without Water

Product	Without water			With 10% water		
	$m^a$	$n^b$	Range of propene concentration	$m$	$n$	Range of propene concentration
Acetaldehyde	0.8	0.32	Up to 20%	0.40	0.49	Up to 20%
Acrolein	0.62	0.47	Up to 10%	0.21	0.5	Up to 20%
Acrolein		0 or negative	10 to 20%	0.32	0.45	Up to 20%
CO <sub>2</sub>	0.62	0.39	Up to 20%	0.32	0.45	Up to 20%

<sup>a</sup> Order with respect to O<sub>2</sub> concentration.

<sup>b</sup> Order with respect to propene concentration.

and without water in the feed. A large increase in propene consumption is observed (Fig. 5) compared to a dry feed. Furthermore, with a dry feed, the propene consumption is reactant inhibited at concentrations higher than 10% propene (at 10% oxygen) whereas, below this concentration, the rate of propene consumption is close to half order with respect to propene. In the presence of water, for the three levels of oxygen investigated, propene is not self-inhibiting and a half-order dependence is observed over the range of propene concentrations employed. Moreover, from the data given in Fig. 5, it is apparent that the rate of propene consumption depends on O<sub>2</sub> concentration; however, the order is less than one-half.

The changes in reaction order for reaction products discussed above are summarized in Table 1. To interpret these measurements, we assume a redox mechanism. For such a mechanism, if the reaction is controlled by catalyst reduction, an  $n$ th-order dependence on propene and a zero-order dependence on oxygen should be expected; if the reaction is controlled by catalyst oxidation, a zero-order dependence on propene and  $m$ th-order dependence on oxygen should occur.

Partial oxidation seems to be controlled by reoxidation of the catalyst in the absence of water when the C<sub>3</sub><sup>2-</sup>/O<sub>2</sub> ratio is greater than unity. Under this condition, the reaction order with respect to propene changes from half to zero or less. Also at this condition, Fig. 4 indicates that water addition produces the largest increase in catalyst activity. With water present in the feed, no change is observed in the reaction order as propene increases to C<sub>3</sub><sup>2-</sup>/O<sub>2</sub> > 1. Furthermore, with the addition of water, the reaction order for the formation of acrolein with respect to oxygen drops from 0.62 to 0.21. A similar change is observed for other products. Therefore, we can conclude that water increases the catalyst activity by enhancing the rate of catalyst reoxidation. However, the mechanism for this enhancement is not indicated by our experiments. The TPD experiments discussed later suggest that there are two types of active sites (I and II) on the vanadate catalyst. Both take part in the

production of acrolein, whereas total oxidation and acrylic acid formation is associated with the type II sites. Because water affects acrylic acid as well as CO<sub>2</sub> production, it must be through the type II sites that water affects activity and selectivity.

#### Step-Change Experiments

These experiments were performed by following the rate of formation of reaction products with time after an abrupt change in the concentration of one component of the reaction mixture. Total flow rate was held constant by varying the flow rate of the nitrogen diluent. Typical transient response curves for a step-up and a step-down in water concentration are shown in Fig. 6 as previously described (33) in a more comprehensive discussion of our transient experiments. To compress the data onto a single plot, the experimental data points have been normalized by dividing the transient concentrations by the product concentrations at steady state. The responses for acrylic acid, acetic acid, and acetaldehyde for a step-up (Fig. 6a) are characterized by a sharp overshoot at the switching point. This overshoot lasts for ca. 2 min. Carbon dioxide formation, however, drops rapidly within the same time interval. Evidently, some of the CO<sub>2</sub> formed at steady state must arise from the total combustion of a strongly surface-bonded acrylic acid, an intermediate for this acid, and possibly carbon scission products (i.e., acetaldehyde and acetic acid) that are present on the catalyst surface in absence of water in the system. Probably the organic acids compete with water for the same adsorption sites. Acetaldehyde on the step-up shows almost no drop when water is switched on and there is complete recovery within 20 min. The different responses of acetaldehyde and CO<sub>2</sub> may mean that water adsorption interferes with the oxidation of the C<sub>1</sub> species formed from the C–C bond scission. CO or H<sub>2</sub>CO may form in place of CO<sub>2</sub> during an interval of several tens of seconds. Acrolein responds to the water step-up by a monotonic increase in concentration until a steady state is reached after about 40 min. No overshoot is observed.

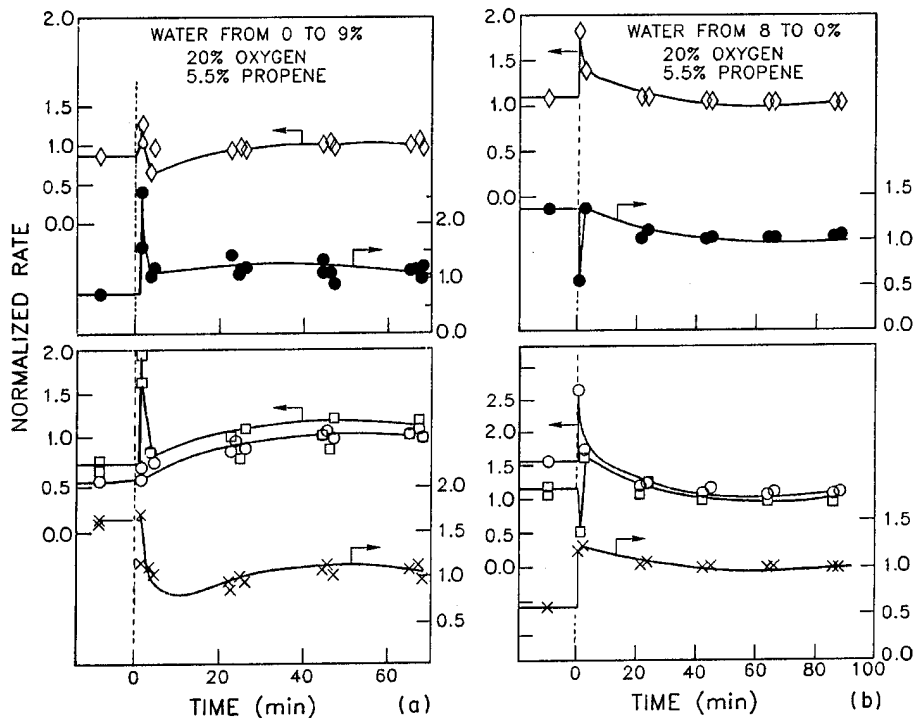


FIG. 6. Transient rate of formation of reaction products at 20% O<sub>2</sub> and 5.5% propene for a step change in water concentration from: (a) 0 to 9%, (b) 8 to 0% at 340°C. (33). Symbols as in Fig. 2.

A rapid rise in product concentration within seconds signals, we believe, adsorption/desorption phenomena. Furthermore, in Fig. 6a the instantaneous exit concentrations for acetaldehyde are below the initial values after the overshoot disappears; for other products, there is a local minimum and concentrations then slowly increase. These observations point to water displacement of oxygenates on the surface (except acrolein) and inhibition of product formation by water adsorption, at least initially. The slow increase in concentration that follows, requiring 40 min, can be explained by surface reorganization or changes in cation valence or coordination extending deeply below the catalyst surface. We hypothesize that the concentration increases can be attributed to the slow generation of new active sites as a result of water adsorbed on the catalyst surface. Perhaps these are nascent sites, unable to function in the absence of water because they are blocked by strongly bonded acids and acetaldehyde species. These blocking species must desorb before these sites can be activated. Desorption is observed after the admission of water vapor, as manifested by the sharp peaks observed in Fig. 6a.

The transient response for a step-down in the water vapor volume percentage from 8 to 0% is shown in Fig. 6b. Each group of products, aldehydes (acrolein and acetaldehyde), acids (acrylic acid and acetic acid), and CO<sub>2</sub>, responds differently. The aldehydes exhibit a sharp overshoot at the switching point ( $t = 0$ ) lasting for ca. 2 min. The maximum is about twice as high as the initial steady-state concentration.

In the same time interval, the acids exhibit a sharp minimum at the switching point. This undershoot disappears in about 2 min.

The sharp overshoot of the acrolein observed in Fig. 6b may be explained by a rapid desorption of water from the catalyst surface, following the sudden reduction of water concentration in the gas phase. This exposes sites for propene adsorption; propene adsorbed on these sites is rapidly transformed into acrolein. Possibly, these sites are particularly active for the formation of acrolein. Whatever the case may be, the sites are reduced as acrolein forms; their regeneration through reoxidation by gaseous oxygen proceeds at a rate much slower than the rate at which acrolein is formed. This leads to the fast decline in acrolein formation within the first 2 min after the step change.

Carbon dioxide responds to the step-down by an overshoot that is weaker than that observed for the partially oxygenated products in Fig. 6b. After this fast transient, a slow relaxation, lasting for about 40 min, is observed. This slow decrease in concentration leaving the reactor is observed for all products.

Except for CO<sub>2</sub>, the steady-state concentrations are below their initial values. There has been, it seems, a loss of active sites. Possible mechanisms include reorganization of the surface, reduction extending below the catalyst surface, or a slow poisoning by a build-up of the product acids. The local maximum in the normalized acrylic acid concentration following the sharp undershoot indicates that a condition

is created on the surface favorable to the formation of the acid. This may signal the availability of acrolein, a precursor for the acid. Evidence for this is that the acrylic acid maximum follows the acrolein maximum by less than a minute.

Transient experiments with  $C_3^{2-}$  and  $O_2$  step changes were also performed. These are discussed in a companion paper (33) but provide no further insight into the role of water.

#### Temperature-Programmed Desorption (TPD)

All measurements were made on catalyst samples pretreated in air for at least 1 h at 460°C. After adsorption of a test species on the catalyst at a chosen temperature, the catalyst was flushed with helium. Desorption was observed using a FID at a heating rate of 10°C/min. Identification of the desorbed materials was made by trapping and injecting samples into a chromatograph. Details and a discussion of the experimental results are to be found elsewhere (33).

The response obtained for two separate experiments with adsorption of propene or acrolein on the catalyst are presented in Fig. 7a. The product analysis for desorption of the propene pulse is given in Fig. 7c. This figure shows that peak I with a maximum at ca. 210°C is composed mainly of acrolein. Small amounts of propene and acetaldehyde are also present. Peak II in Fig. 7a has a maximum at ca. 320°C and is composed of a mixture of acetaldehyde, propene, acrylic and acetic acids, and acrolein. As may be seen from

the figure, acids desorb only above 300°C, indicating either they are strongly adsorbed on the catalyst surface or that the activation energy is high for their formation from a surface precursor. Much of the catalyst surface ought to be covered with adsorbates based on the observed peak II near 340°C, the temperature at which our steady-state and step-change experiments were conducted. Apparently there are two sets of active sites. One corresponds to peak I in Fig. 7a and is referred to as type I sites. Propene abstracts oxygen to form acrolein on these sites. Once the surface is reduced, we hypothesize that these sites are no longer capable of chemisorbing propene. A second type (II) strongly adsorbs propene. Most of the acrolein originates from type I sites which can be characterized as weakly adsorbing at the reaction temperature, whereas acrylic acid forms on the type II sites. There may be diffusion of acrolein from type I to type II sites. Total oxidation probably occurs only on type II sites. We surmise that the degree of oxidation or rather cation coordination of the vanadate surface controls the distribution of adsorbates: at a high degree of oxidation, acrylic acid or acrolein predominates, whereas on a reduced surface, propene predominates.

Some acetaldehyde appears to originate with the first set of sites, but the acetaldehyde peak in Fig. 7c probably means that most C-C bond scission occurs on the strong adsorption sites. Acrolein adsorption occurs rapidly on the type I sites as may be seen in Fig. 7a; adsorption on the

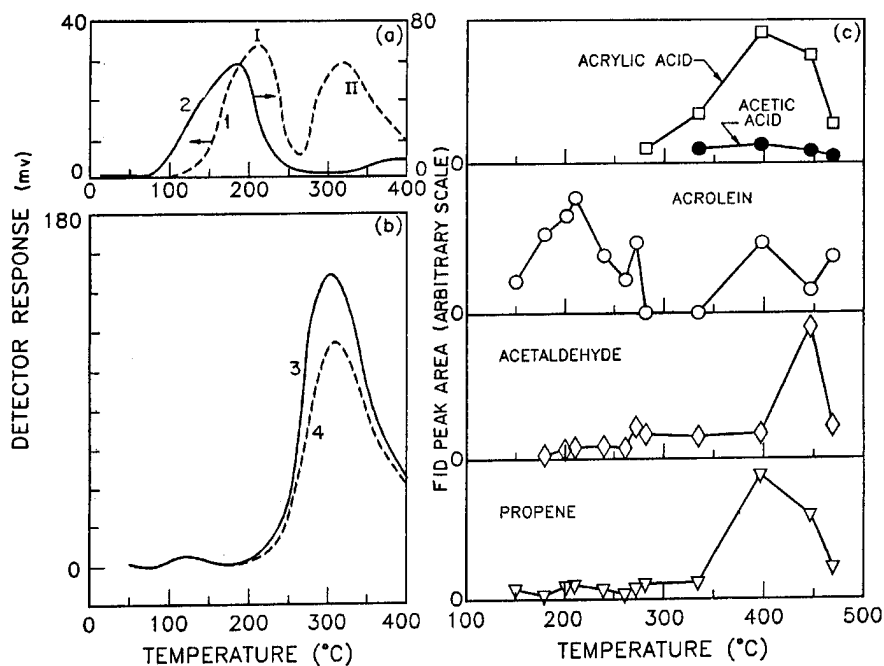


FIG. 7. Signal and peak composition vs temperature in TPD (33). (a) Thermal conductivity signal after adsorption of propene from a He carrier at 150°C (curve 1, --) and after adsorption of acrolein from a He carrier at 150°C (curve 2, —), (b) thermal conductivity signal after adsorption of propene from a He carrier at 200°C with no preadsorption of water (curve 3, —) and after adsorption of propene with preadsorption of water (curve 4, --), (c) chromatograph analysis (FID) of the composition of the TCD signal in (a) for propene adsorption at 150°C. Symbols as in Fig. 2.



oxidized type II sites appears to be limited. The small peak between 350 and 400°C in Fig. 7a is probably acrylic acid so that any acrolein adsorbed is further oxidized to this acid. The TPD results suggest the rate of acrylic acid formation may be desorption limited.

Because type II sites seem to be associated with acrylic acid formation, C–C scission, and probably total oxidation, the role of water in adsorption was explored by adsorbing  $C_3^{2-}$  at 200°C in the presence and absence of water vapor. Figure 7b shows the results. Peak II is substantially reduced by preadsorption of water. Apparently, water competes with propene for the strong adsorption sites.

### Isotopic Transients

The experimental measurements using  $^{18}O_2$  with the Sb/Sn/V oxide catalyst were carried out at the University of Pittsburgh. When water vapor was added to the feed, a level of 0.4% was used. This level showed the largest effect on product distribution at 340°C. Experimental details and the results obtained are dealt with in a companion article (33). Only results pertinent to the role of water in propene partial oxidation are discussed in what follows.

Transient responses for acrolein, acetaldehyde, and  $CO_2$  isotopes were observed following a switch from  $^{16}O_2$  to  $^{18}O_2$  under reaction conditions. Acrylic acid was not detected at the low conversions used. Results for the  $CO_2$  isotopes are displayed in Fig. 8. Replication of the experiment without water shows good reproducibility. The  $C^{16}O_2$  signal decays slowly with respect to He tracer and reaches zero after about 4 min. This indicates either strongly adsorbed  $CO_2$  or formation from a hydrocarbon/lattice oxygen reaction. The response of  $C^{16}O^{18}O$  passes through a maximum at ca. 0.3 min, and then decays slowly. In the first 12 s, the signal for  $C^{18}O_2$  increases at about half the rate for  $C^{16}O^{18}O$ . A very slow or restricted exchange of gas-phase oxygen with lattice oxygen would imply a direct oxidation of adsorbate to  $CO_2$  with gas-phase or adsorbed  $O_2$ . However, this direct route to  $CO_2$  must be less important than further oxidation of partially oxygenated species, judging from the smaller slope of the  $C^{18}O_2$  response relative to that of  $C^{16}O^{18}O$  in the first 12 s.

The  $C^{16}O_2$  response (Fig. 8b) reaches zero much faster with water vapor in the feed than in its absence (Fig. 8a). Lower coverage of the surface by  $CO_2$  and/or other adsorbates explains this observation. The concentration ( $C^{16}O^{18}O$ ) was twice as high as that observed in the absence of water vapor and did not show a noticeable decay during the time of the experiment. This suggests the existence of a constant source of  $^{16}O$ , presumably from water vapor present in the feed of the reactor. In the absence of water, a slow decay in the formation of  $C^{16}O^{18}O$  is observed (see Fig. 8a), and is attributed to the slow depletion of the  $^{16}O$  from the catalyst. This observation suggests that oxygen from water exchanges with the surface or can be incorporated into a surface intermediate that can be further oxidized to  $CO_2$ .

The responses of acrolein and acetaldehyde for these experiments are discussed elsewhere (33). They suggest that acrolein must be partially formed from lattice oxygen or oxygen adsorbed on the vanadate surface. If it is lattice oxygen, the results are consistent with the TPD measurements which suggest that it forms on type I sites. Acetaldehyde behaved like acrolein, which suggests that the carbon bond scission may occur to a larger extent on the type II sites than the TPD measurements implied.

To test the hypothesis that water participates in acrylic acid formation, the  $H_2^{18}O$  response was measured for an isotope switch in the presence of 0.4% water and is shown in Fig. 9. This concentration of water vapor was chosen because, as Fig. 4 shows, acrolein formation reaches a maximum at this concentration. The increase of  $H_2^{18}O$  was very slow compared to the  $CO_2$  isotopes shown in Fig. 8. Over 480 s was needed to reach steady state. Water exchange with adsorbed oxygen on the catalyst surface or with lattice oxygen of the fully oxidized vanadate is indicated; however, it is also possible that the slow build-up was caused by water adsorption in the mass spectrometer. If the slow build-up results solely from exchange, it is small compared to the rates of other steps; thus, the transfer of  $^{16}O$  to acrylic acid from the catalyst to acetic acid and eventually to the  $C^{16}O^{18}O$  observed must be unimportant. Evidently, adsorbed water participates directly in the formation of acrylic acid.

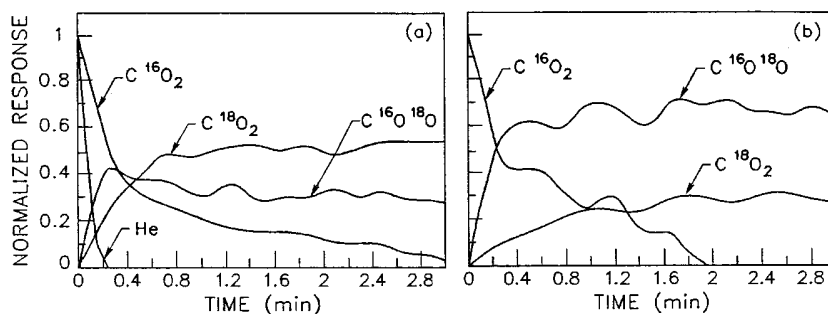


FIG. 8. Isotopic transient response of  $CO_2$  under reaction conditions at 20%  $O_2$  and 5% propene following an isotopic switch in oxygen from mass 32 to 36 at 340°C. (a) No water in the feed, (b) 0.4% water in the feed.

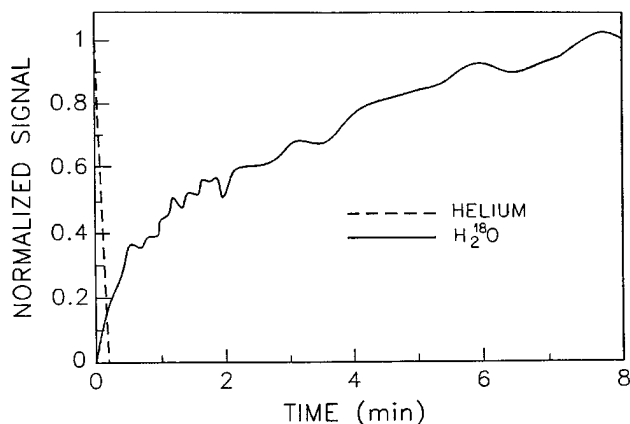


FIG. 9. Isotopic transient response of water  $\text{H}_2^{18}\text{O}$  without reaction after switching from  $^{18}\text{O}_2$  in the presence of water ( $\text{H}_2^{16}\text{O}$ ) at  $340^\circ\text{C}$ .

Another contribution could be an exchange reaction between adsorbed water and adsorbed  $\text{CO}_2$ , since both compounds spend a relatively long time on the catalyst surface. However, the slow exchange between water and surface means that this mechanism can make only a small contribution.

The average residence time of a species on the catalyst surface can be estimated from the response (33). The residence time of water for the response shown in Fig. 9 was ca. 116 s, which is three greater than the residence time observed under reaction conditions. This indicates an abundance of  $^{18}\text{O}$  on the surface in the absence of propene. Dissociative adsorption of water on the catalyst surface is probably necessary for exchange. The rate of this step, i.e., the strength of the adsorption bond, may depend on the condition of the surface. Differences between the oxidized surface for the experiment shown in Fig. 9 and the presumably partially reduced surface under reaction conditions may also explain the residence times observation. It may also explain the discrepancy between the report of a rapid exchange reaction between water and oxide catalyst by Nováková *et al.* (34) and our own observation.

## DISCUSSION

We speculate on the role of water vapor using a mechanism developed by Grabowski *et al.* (35) from their IR study of acrolein adsorption on cobalt molybdate. According to these researchers, acrolein exists on the mixed oxide surface as  $\pi$ -bonded complex or as a species bonded via the carboxylic oxygen to a metal in the surface. These two surface species may be in equilibrium or at least the transformation from one to the other proceeds rapidly. The  $\pi$ -bonded species reacts with surface oxygen through the carboxylic carbon to yield the surface precursor of acrylic acid. On the other hand, the oxygen-bonded species undergoes a nucleophilic attack by adjacent surface oxygen to form a bridge-bonded complex. Grabowski *et al.* (35) provide spectro-

scopic evidence for these intermediates. The bridge-bonded complex presumably reacts further with nearby adsorbed or lattice oxygen to yield total oxidation products. We propose that water vapor competes for sites at which carboxylic oxygen bonds to the cation, greatly lowering the probability of oxygen on the surface adjacent to the bridge-bonded complex. The lower probability of nearby oxygen reduces further oxidation of the complex or possibly even its formation. This could account for the behavior seen in Fig. 4.

Competition between adsorbed water and precursors of acrylic acid for the same sites leads to displacement of acrylic acid from the surface as water vapor enters the feed. Water adsorption does not occur at  $340^\circ\text{C}$  on the sites for the  $\pi$ -bonded complex (these were the type I sites in our TPD results), so acrolein production is only slightly affected. This conforms to the experimental observations in Fig. 6a. The rise in the rate of formation of all products after the initial transients is assumed to be a separate process, as discussed earlier in this paper. It is conceivable that strongly adsorbed bridge-bonded complex reduces the number of sites for acrylic acid formation (these were identified as type II sites in our TPD study). The slow displacement of the bridge-bonded complex by water may make these sites available for acrolein and acrylic acid formation and/or C-C splitting to yield acetaldehyde, thus accounting for the gradual rise in catalyst activity that is shown after 2 to 3 min in Fig. 6a.

When water vapor is removed from the feed, the surface steady state is disturbed. Water desorption opens up sites for propene and acrylic acid adsorption. This results in an immediate drop in acrylic acid desorption from the surface. Adjacent oxygen sites on the surface increase, leading to a rise in  $\text{CO}_2$  production. Because acrolein appears to be an intermediate in propene oxidation to acrylic acid, acrolein production would be expected to show a sharp rise, followed by a decline as acrolein is converted to acrylic acid or is further oxidized to  $\text{CO}_2$  and water. The acrolein peak followed closely by an acrylic acid peak can be seen in Fig. 6b. The slow decrease in the concentration of all products after peaks may be attributed, perhaps, to a slow build-up of the strongly adsorbed bridge-bonded complex.

## ACKNOWLEDGMENTS

Support for this project came from operating grants given by the Natural Sciences and Engineering Research Council of Canada to two of us (R.R.H. and P.L.S.). We are grateful for a fellowship from the Government of Saudi Arabia to Y.A.S.-A. Professor James Goodwin, University of Pittsburgh, generously permitted us to use his isotopic transient equipment and guided our experiments. Professor K. Muira, Kyoto University, Japan, built our TPD unit and provided instruction in its use.

## REFERENCES

1. Sakuyama, S., Ohara, T., Shimizu, N., and Kubota, K., *Chem. Tech.* June, 350 (1973).

2. Nováková, J., Dolejšek, Z., and Habersberger, K., *React. Kinet. Catal. Lett.* **43**, 389 (1976).
3. Adams, C. R., and Jennings, T. J., *J. Catal.* **2**, 63 (1963).
4. Adams, C. R., and Jennings, T. J., *J. Catal.* **3**, 549 (1964).
5. Sachtler, W. M. H., and De Boer, N. H., in "Proceedings, 3rd International Congress on Catalysis, Amsterdam, 1964" (W.M.H. Sachtler, G.C.A. Schuit, and P. Zwietering, Eds.), Vol. 1, p. 253. Wiley, New York, 1965.
6. Godin, G. W., McCain, C. C., and Porter, E. A., in "Proceedings, 4th International Congress on Catalysis, Moscow, 1968" (B.A. Kazansky, Ed.), p. 271. Adler, New York, 1968.
7. Ono, T., Hillig II, K. W., and Kuczkowski, R. L., *J. Catal.* **123**, 236 (1990).
8. Imachi, M., Kuczkowski, R. L., Groves, J. T., and Cant, N. W., *J. Catal.* **82**, 335 (1983).
9. Margolis, L. Ya., *Catal. Rev. Sci.-Eng.* **82**, 241 (1973).
10. Haber, J., and Grzybowska, B., *J. Catal.* **28**, 489 (1973).
11. Haber, J., in "Proceedings, 8th International Congress on Catalysis Berlin 1984" Vol. 1, p. 85. Dechema, Frankfurt-am-Main, 1984.
12. Ueda, W., Moro-oka, Y., and Ikawa, T., *J. Catal.* **88**, 214 (1984).
13. Wragg, R. D., Ashmore, P. G., and Hockey, J. A., *J. Catal.* **22**, 49 (1971).
14. Sancier, K. M., Wentreck, P. R., and Wise, H., *J. Catal.* **39**, 141 (1975).
15. Ruckenstein, E., Krishnan, R., and Rai, K. N., *J. Catal.* **45**, 270 (1976).
16. Monnier, J. R., and Keulks, G. W., *J. Catal.* **63**, 51 (1981).
17. Garnish, A. M., Shafranskii, L. M., Skvortsov, N. P., Zvezdina, E. A., and Stepanovskaya, V. F., *Kinet. Katal.* **32**, 220 (1962). [In English]
18. Gorokhovatskii, Ya. B., and Popova, E. N., *Kinet. Katal.* **51**, 111 (1962). [In English]
19. Polkovnikova, A. G., Kruzhalov, B. D., Shatalova, A. N., and Tseitina, L. I., *Kinet. Katal.* **32**, 216 (1962). [In English]
20. Boreskov, G. K., Erenburg, E. M., Andrushkevich, T. V., Zelenkova, T. V., Bibin, V. N., Meshcheryakov, V. D., Boronina, N. P., and Tyurin, Yu. N., *Kinet. Katal.* **23**, 755 (1982). [In English]
21. Svachula, J., Tockstein, A., and Tichy, J., *React. Kinet. Catal. Lett.* **31**, 187 (1986).
22. Arnold III, E., and Sundaresan, S., *Appl. Catal.* **14**, 225 (1988).
23. Moro-oka, Y., Takita, Y., and Ozaki, A., *J. Catal.* **27**, 177 (1972).
24. Moro-oka, Y., Ohata, T., Takita, Y., and Ozaki, A., *Bull. Chem. Soc. Jpn.* **46**, 681 (1973).
25. Portefaix, J. L., Figueras, F., and Forissier, M., *J. Catal.* **63**, 307 (1980).
26. Seiyama, T., Yamazoe, N., and Egashira, M., in "Proceedings, 5th International Congress on Catalysis, Palm Beach, 1972" J. W. Hightower, Ed.), Vol. 2, p. 997. North-Holland, Amsterdam, 1973.
27. Saleh, Y. A. A., Ph.D. thesis, University of Waterloo, Chemical Engineering Department, Waterloo, Ontario, Canada, 1990.
28. Hudgins, R. R., *Chem. Eng. Sci.* **23**, 93 (1968).
29. Hudgins, R. R., *Can. J. Chem. Eng.* **50**, 427 (1972).
30. Mears, D. E., *J. Catal.* **20**, 127 (1971).
31. Anderson, J. B., *Chem. Eng. Sci.* **18**, 147 (1963).
32. Volta, J. C., Bussière, P., Coudurier, G., Herrmann, J. M., and Védrine, J. C., *Appl. Catal.* **16**, 315 (1985).
33. Saleh-Alhamed, Y.A.A., Hudgins, R. R., and Silveston, P. L., *Appl. Catal. A* **127**, 177 (1995).
34. Nováková, J., Jířů, P., and Zavadil, V., *Coll. Czech. Chem. Commun.* **37**, 1233 (1972).
35. Grabowski, R., Haber, J., and Sloczynski, J., *React. Kinet. Catal. Lett.* **12**, 119 (1979).